Structural and magnetic properties of $ErFe_2D_5$ studied by neutron diffraction and Mössbauer spectroscopy



2003 J. Phys.: Condens. Matter 15 4349

(http://iopscience.iop.org/0953-8984/15/25/306)

INSTITUTE OF PHYSICS PUBLISHING JOURNAL OF PHYSICS: CONDENSED MATTER

J. Phys.: Condens. Matter **15** (2003) 4349–4359 PII: S0953-8984(03)61014-3

# Structural and magnetic properties of $ErFe_2D_5$ studied by neutron diffraction and Mössbauer spectroscopy

**V Paul-Boncour[1,5], S M Filipek[2], I Marchuk[2], G André[3], F Bourée[3], G Wiesinger[4] and A Percheron-Guégan[1]**

[1] Laboratoire de Chimie Métallurgique des Terres Rares, CNRS, 2-8 rue H Dunant, 94320 Thiais, France
[2] Institute of Polish Chemistry PAN, Ulica Kasprzaka 44/52, 01224 Warsaw, Poland
[3] Laboratoire Léon Brillouin, CEA-CNRS, CEA/Saclay, 91191 Gif/Yvette, France
[4] Institute for Solid State Physics, Vienna University of Technology, Wiedner Hauptstrasse 8-10/131, A-1040 Vienna, Austria

E-mail: paulbon@glvt-cnrs.fr

Received 18 March 2003, in final form 22 May 2003
Published 13 June 2003
Online at stacks.iop.org/JPhysCM/15/4349

**Abstract**

A neutron powder diffraction study of $ErFe_2D_5$, synthesized under 1 GPa hydrogen pressure, shows that it crystallizes at room temperature in an orthorhombic structure described by the $Pmn2_1$ space group with $a = 5.42$ Å, $b = 5.79$ Å, $c = 8.00$ Å. The deuterium atoms order preferentially in some $A_2B_2$ and $AB_3$ interstitial sites. Below 5 K the erbium moments order in a canted magnetic structure, with an erbium moment of 6.6 $\mu_B$ at 1.4 K. The $^{57}$Fe Mössbauer spectra of $ErFe_2D_5$ from 4.2 to 300 K indicate that there are no ordered Fe moments at zero field. These results are discussed in relation to the influence of hydrogen absorption on the magnetic interactions.

## 1. Introduction

The $RFe_2$ compounds (R = Y, rare earth) display a multiplateau behaviour in their pressure–composition isotherms [1, 2]. This multiplateau behaviour has been related to the formation of hydrides with different structures due to deuterium order below a critical temperature [3–5]. The $ErFe_2H_x$ hydrides crystallize at room temperature in a cubic C15 type structure up to $x = 3.5$, in a rhombohedral structure for $x = 3.6$–$3.7$ [3, 6–8] and again in a cubic C15 structure for $x = 4.0$ [9]. Applying a high hydrogen pressure leads to the formation of $ErFe_2H_5$ which crystallizes at room temperature in an orthorhombic structure with a relative cell volume increase of nearly 30% [9, 10]. The influence of hydrogen absorption in the magnetic properties of $RFe_2$ has been widely studied. For low H content ($x \leqslant 3.6$) the hydrides are ferri- or ferromagnetic, depending on the R element [8, 11, 12]. For most of the $RFe_2$ hydrides

[5] Author to whom any correspondence should be addressed.

  

both the Curie temperature $T_C$ and the compensation temperature $T_{comp}$ decrease as the H content increases, indicating a weakening of the magnetic exchange interactions [3, 8, 13]. Studies of the $ErFe_2H_x$ hydrides by Mössbauer spectroscopy indicated an increase of the mean Fe moment up to $x = 3.6$ and a sharp decrease for $x = 4.1$ [14]. A fanning of the Er moments was also observed and attributed to a non-collinear orientation of the Er and Fe moments due to the hydrogen distribution [11, 14]. The previous study of the magnetic properties of $ErFe_2H_5$ has revealed a weak magnetization down to 100 K and a sharp increase below 50 K which was attributed to the ordering of Er moments [9, 15].

In this work we present neutron powder diffraction (NPD) experiments, magnetic and $^{57}$Fe Mössbauer spectroscopy measurements performed in order to clarify the nuclear and magnetic structures of $ErFe_2D_5$. These results will be discussed in relation to the previous ones on the $ErFe_2$–$H_2$ system with the aim of improving the understanding of the influence of large H (D) content on the magnetic interactions in such systems.

## 2. Experimental details

The $ErFe_2$ intermetallic compounds were synthesized by induction melting of the pure elements (Er 99.9% and Fe 99.99%) followed by an annealing treatment under vacuum over three weeks at 943 K. The samples were found to be single-phase and homogeneous with a C15 cubic structure and a cell parameter $a = 7.28$ Å. Small pieces of $ErFe_2$ were placed in a piston–cylinder high pressure apparatus and outgassed for 16 h at 100 °C. Then the hydrogen or deuterium gas was purified on a Pt bed and compressed to 100 MPa with a pressure intensifier. Further compression from 0.2 to 1.1 GPa was performed by using a hydraulic press of 100 t capacity. The temperature of the high pressure apparatus was kept constant at 100 °C by using a conventional temperature control system. After 25 days of hydrogen exposure, the samples were quenched and kept in liquid nitrogen until characterization could be performed.

The x-ray diffraction (XRD) patterns were measured with a D8 Brucker diffractometer in the range $10° < 2\theta < 120°$ with a stepwidth of 0.02° using Cu K$\alpha$ radiation. The NPD patterns of the deuteride were recorded at 10 and 270 K on the 3T2 diffractometer and from 1.4 to 300 K on the G4.1 diffractometer in the Laboratoire Léon Brillouin (LLB) at Saclay. For the 3T2 experiment the wavelength was 1.225 Å and the angular range $6° < 2\theta < 125°$ with a step of 0.05°. For the G4.1 experiments the wavelength was 2.427 Å and the angular range was $2° < 2\theta < 82°$ with a step of 0.1°. The deuteride sample was contained in a vanadium sample holder. All the XRD and NPD were refined with the Rietveld method, using the Fullprof program [16].

The magnetic measurements were performed from 4.2 to 420 K with a DSM8 Manics magneto-susceptometer for applied fields up to 1.8 T.

The $^{57}$Fe Mössbauer spectra were recorded between 4.2 and 300 K using a conventional constant acceleration type spectrometer with a $^{57}$Co(Rh) source. The isomer shift data are given relative to the source (Fe(Rh)).

## 3. Results and discussion

### *3.1. Hydride and deuteride synthesis and stability*

In order to determine the most appropriate conditions for the $ErFe_2H_x$ hydride synthesis, the applied hydrogen pressure was varied between 0.2 and 1.1 GPa at $T = 100$ °C. The analysis of the XRD patterns from the resulting compounds showed a mixture of cubic and orthorhombic phases, corresponding to $x \approx 4$ and 5, respectively, in agreement with [9]. The

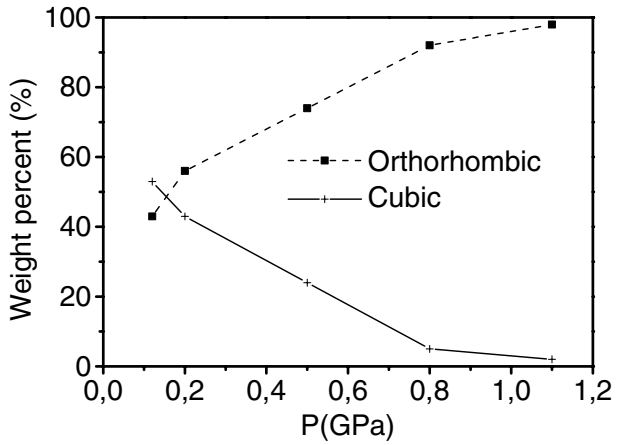


**Figure 1.** Evolution of the weight percentage of cubic $ErFe_2D_4$ and orthorhombic $ErFe_2D_5$ versus applied hydrogen pressure.

weight percentage of the orthorhombic phase increased at the expense of the cubic phase as the hydrogen pressure was raised (figure 1), reaching nearly 100% for 1.1 GPa. In [9] the authors stated that the orthorhombic phase can be obtained under a pressure of only 5.3 MPa after 48 h at 273 K, but it is absolutely necessary to poison the surface with carbon disulfide in order to keep it for a few days. In our experiments, no chemical sealing of the surface by carbon disulfide or any other poison was performed after H or D absorption, but a pressure as large as 1.1 GPa was necessary to stabilize $ErFe_2D_5$. It is noticeable that in this case we observed only a small decrease of the cell parameters, without an increase of the cubic phase contribution and after keeping it for 3 weeks at room temperature and under atmospheric pressure.

### *3.2. Structural and magnetic properties*

In [10] the XRD pattern of $ErFe_2H_5$ at 290 K was refined in a centred orthorhombic structure described in the $Imm2$ space group (SG) with $a = 5.424(1)$ Å, $b = 5.793(1)$ Å and $c = 8.009(1)$ Å. The analysis of the XRD pattern of the $ErFe_2D_5$ sample used for NPD indicates 95% of the orthorhombic phase ($ErFe_2D_5$) with $a = 5.407$ Å, $b = 5.776$ Å and $c = 7.987$ Å and 5% of the cubic C15 phase ($ErFe_2D_4$) with $a = 7.877$ Å. The corresponding NPD pattern measured at 270 K shows additional lines which can be indexed in a primitive orthorhombic cell with the extinction of $00l$, $h00$ and $h0l$ lines when $h$, $l$ and $h + l$ are odd. Among the three available primitive subgroups of $Imm2$: $Pnn2$, $Pmm2$ and $Pmn2_1$, the $Pmn2_1$ SG was found to be the most appropriate to refine the NPD pattern, taking into account the observed extinctions. A shift of the origin of (0, 1/4, 0), i.e. a shift of 0.25 of the $y$ coordinates, compared to the description in the $Imm2$ SG is necessary to describe the atomic positions. In this description there are two Er (A atom) and three Fe (B atom). In the C15 cubic structure the hydrogen atom can be located in three different types of interstitial tetrahedral site: one $A_2B_2$ site (2 Y and 2 Fe neighbours) with 96 equivalent positions, the $AB_3$ site (1 Y and 3 Fe) with 32 equivalent positions and one $B_4$ site (4 Fe) with 8 equivalent positions. Due to the lowering of crystal symmetry from cubic to orthorhombic structure these sites are split into fourteen $A_2B_2$, six $AB_3$ and two $B_4$ interstitial sites. In order to determine the most probable sites occupied by a D atom, the '*ab initio* crystal structure solution from diffraction data' code Fox (free object for crystallography) [17] was used before running the Fullprof

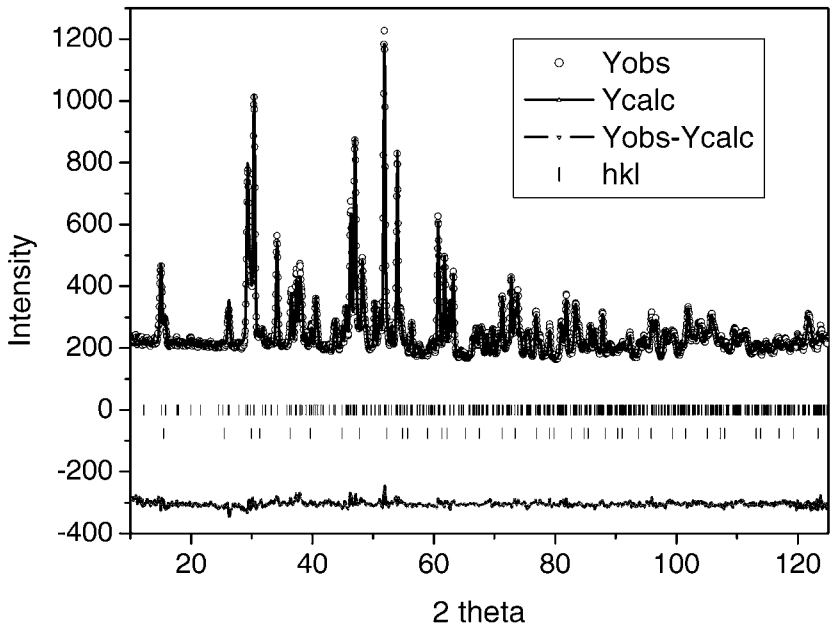


**Figure 2.** Refined NPD pattern of a $ErFe_2D_5$ compound measured on the 3T2 spectrometer at 270 K. The upper *hkl* bars correspond to the orthorhombic phase and the lower ones to the cubic $ErFe_2D_4$ phase.

code [16]. The refined parameters are reported in table 1 and the corresponding refined pattern at 270 K in figure 2. The analysis of the 270 K diffraction data shows that only 6 $A_2B_2$ ($D_1$–$D_6$) and 2 $AB_3$ ($D_7$ and $D_8$) sites are fully or partially occupied by deuterium atoms, whereas the $B_4$ sites are empty. The fact that the $D_1$ and $D_2$ sites are only half occupied is in agreement with the existence of very short $D_1$–$D_1$ (0.473 Å) and $D_2$–$D_2$ distances (0.777 Å), which excludes one D atom over two in these two sites, due to repulsive interactions between D atoms. All the other D–D distances are equal to or larger than 2.10 Å, which corresponds to the minimum D–D distance according to the Switendick criterion [18]. The Fe–D and Er–D distances are close to or larger than the sum of the atomic radii of the Fe (1.24 Å) or Er atoms (1.76 Å) and the D atom (0.4 Å), in agreement with the general behaviour of metal hydrides. The total content of the refined D atom occupancy of 4.62 D/fu corresponds to a cell volume increase of about 3 $Å^3$/D atom, not far from the 2.8–2.9 $Å^3$/D atom generally observed [19]. If the $D_1$ and $D_2$ sites were half occupied and the $D_3$–$D_8$ sites fully occupied a total D content of 5 D/fu would be reached. At 10 K similar results are obtained, with slight variations in the atomic positions and occupancy factors of the D atoms.

The evolution of selected NPD patterns at different temperatures is displayed in figure 3. The cell parameter variation (figure 4) shows a decrease in *a* and an increase in *b* and *c* from 10 to 300 K. The anomaly of the *a* parameter variation at 300 K can reflect the starting reduction of the orthorhombic distortion since a structural transition from orthorhombic to cubic C15 structure is expected at larger temperatures. Below 10 K a sharp variation of all the cell parameters is observed: it decreases from 10 down to 7 K, increases again with a maximum at 5 K and decrease at lower temperatures. This particular structural behaviour seems to be related to the onset of magnetic order.

Indeed, the comparison of the NPD patterns above and below 5 K indicates the presence of additional lines which can be attributed to the magnetic order of the Er moments. The difference

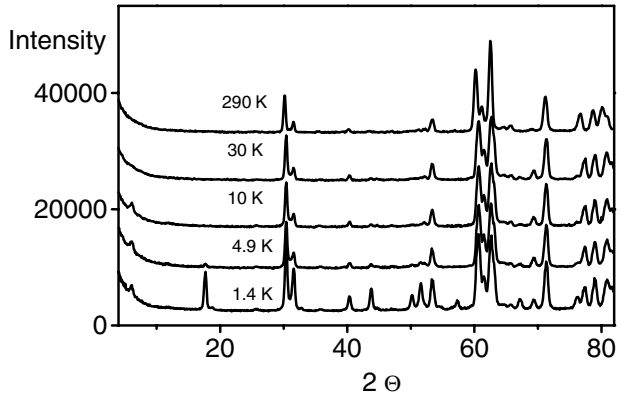


**Figure 3.** Selected NPD of $ErFe_2D_5$ at various temperatures measured on a G4.1 spectrometer.

**Table 1.** Refined cell parameters, atomic positions, thermal factors and deuteride occupancy numbers from the 3T2 NPD pattern of $ErFe_2D_5$ at 270 K. The $D_1$–$D_6$ sites are $A_2B_2$ types interstitial sites and the $D_7$–$D_8$ are $AB_3$ ones.

| Phase 1 | Orthorhombic | SG $Pmn21$ | Fract. = 96.2 (wt%) | | |
|---|---|---|---|---|---|
| $a = 5.398(3)$ Å | $b = 5.770(3)$ Å | $c = 7.979(3)$ Å | $V = 248.53$ Å$^3$ | | |
| Atom | | | | | |
| (Wyckoff) | $x$ ($\delta x$) | $y$ ($\delta y$) | $z$ ($\delta z$) | $B$ ($\delta B$) | $N$ ($\delta N$) |
| Er1(2a) | 0 | 0.258(6) | 0 | 0.48(33) | 1 |
| Er2(2a) | 0 | 0.764(6) | 0.771(3) | 0.44(30) | 1 |
| Fe1(4b) | 0.252(3) | 0.255(3) | 0.636(6) | 0.43(10) | 1 |
| Fe2(2a) | 0 | −0.0260(6) | 0.392(6) | 0.20(30) | 1 |
| Fe3(2a) | 0 | 0.488(6) | 0.382(6) | 0.99(40) | 1 |
| D1(4b) | 0.044(6) | 0.233(9) | 0.275(6) | | 0.53(5) |
| D2(4b) | 0.428 (3) | 0.285(4) | 0.001(6) | | 0.51(5) |
| D3(2a) | 0 | 0.384(9) | 0.712(6) | | 0.97(7) |
| D4(2a) | 0 | 0.882(9) | 0.036(6) | | 0.85(7) |
| D5(4b) | 0.216(6) | 0.584(6) | 0.952(6) | 1.20(12) | 1.00(6) |
| D6(4b) | 0.272(6) | 0.937(6) | 0.304(6) | | 0.79(5) |
| D7(2a) | 0 | 0.072(9) | 0.584(9) | | 0.88(8) |
| D8(2a) | 0 | 0.564(12) | 0.172(9) | | 0.86(9) |
| D(total)/fu | | | | | 4.62 (1) |
| Phase 2 | Cubic | SG $Fd\bar{3}m$ | Fract. = 3.8 (wt%) | | |
| $a = 7.874$ Å | | $V = 488.13$ Å | | | |
| $R_F = 8.6\%$ | $R_{B1} = 5.2\%$ | $R_{B2} = 4.1\%$ | | 533 ind. | reflections |

pattern between 10 and 1.4 K (figure 5) can be refined in a canted magnetic structure with AF coupling along $a$, no component along $b$ and F coupling along $c$ (table 2). The refinement of the pattern at 1.4 K with both magnetic and nuclear contributions leads to a total Er moment of 6.6 $\mu_B$ (table 2). The Er magnetic moment decreases down to $T_C = 5$ K (figure 6). The schematic structure of $ErFe_2D_5$ is presented in figure 7: the arrows represent the orientation of the Er moments below 5 K and among the D atoms the shortest $D_1$–$D_1$ and $D_2$–$D_2$ distances have been indicated.

The appearance of a weak line at $2\theta = 6°$ ($d = 23.3$ Å) is observed for a temperature below 25 K (figure 3). This magnetic line can be related to the second phase $ErFe_2D_4$ since at

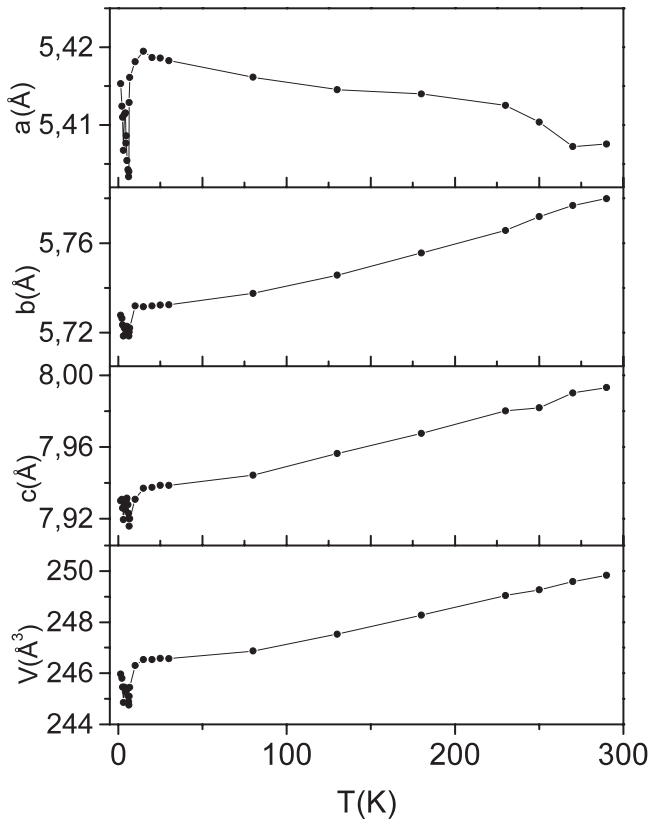


**Figure 4.** Evolution of the orthorhombic cell parameters and cell volume of $ErFe_2D_5$ versus temperature.

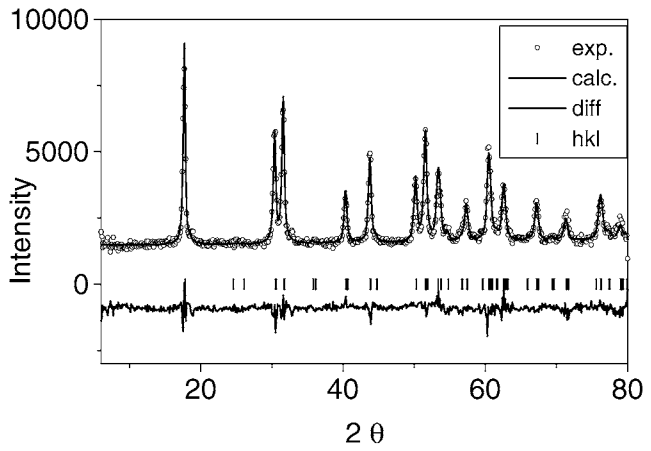


**Figure 5.** Difference neutron diffraction pattern of $ErFe_2D_5$ between 1.4 and 10 K. The refinement was done with the magnetic structure described in table 2.

the same time the intensity of the (111) line of $ErFe_2D_4$ increases significantly as observed in the difference pattern between 5.5 and 30 K. The small angle line is located at $d \approx 3^* a_C$. As

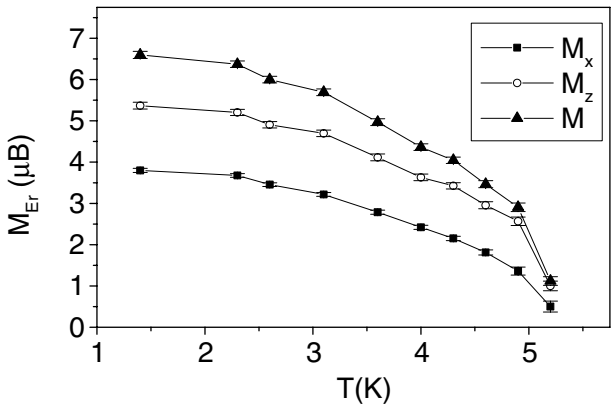


**Figure 6.** Evolution of the Er magnetic moment ($M$) and the $M_x$ and $M_z$ components obtained from the NPD pattern refinement.

**Table 2.** Refined nuclear and magnetic structures at 1.4 K from the G4.1 NPD pattern of $ErFe_2D_5$. The atomic positions have been fixed to the values refined at 10 K on the 3T2 NPD pattern whereas the occupancy factors of the D atoms have been refined. For the cubic '$ErFe_2D_4$' only the nuclear contribution has been refined, but weak non-refined additional lines should be due to the magnetic contribution of this phase.

| Phase 1 | Orthorhombic | SG $Pmn21$ | | |
|---|---|---|---|---|
| $a = 5.418(1)$ Å | $b = 5.732(1)$ Å | $c = 7.936(2)$ Å | $V = 246.46$ Å$^3$ | |
| Atom | | | | |
| (Wyckoff) | $x$ | $y$ | $z$ | $N$ |
| D1(4b) | 0.061 | 0.238 | 0.283 | 0.40 |
| D2(4b) | 0.453 | 0.291 | 0.008 | 0.50 |
| D3(2a) | 0 | 0.375 | 0.727 | 1.00 |
| D4(2a) | 0 | 0.907 | 0.049 | 0.74 |
| D5(4b) | 0.210 | 0.590 | 0.959 | 1.00 |
| D6(4b) | 0.264 | 0.939 | 0.312 | 0.96 |
| D7(2a) | 0 | 0.076 | 0.592 | 1.00 |
| D8(2a) | 0 | 0.558 | 0.176 | 1.00 |
| D(total)/fu | | | | 4.73 (1) |
| Magnetism | $M_x$ ($\mu_B$) | $M_y$ ($\mu_B$) | $M_z$ ($\mu_B$) | $M$ ($\mu_B$) |
| Er1_1 | 3.8(1) | 0 | 5.3(1) | 6.6(2) |
| Er1_2 | −3.8(1) | 0 | 5.3(1) | 6.6(2) |
| Er2_1 | 3.8(1) | 0 | 5.3(1) | 6.6(2) |
| Er2_2 | −3.8(1) | 0 | 5.3(1) | 6.6(2) |
| Phase 2 | Cubic | SG $Fd\bar{3}m$ | | |
| $a = 7.871$ Å | | $V = 488.13$ Å$^3$ | | |
| $R_F = 12.6\%$ | $R_{B1} = 7.3\%$ | $R_{mag} = 7.7\%$ | $R_{B2} = 4.3\%$ | |

the magnetic structure of the cubic $ErFe_2D_4$ phase is not really solved up to now, it was not possible to refine it in the low temperature patterns.

Actually all the $^{57}$Fe Mössbauer spectra shown in figure 8 may be fitted with doublets over the entire range of temperatures experimentally covered (4.2 K $\leqslant T \leqslant$ 295 K). In addition

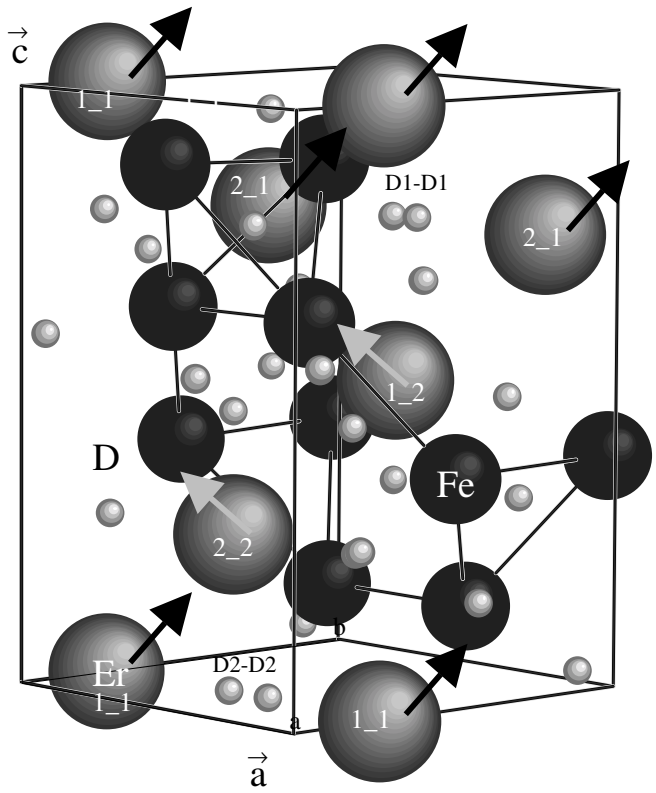


**Figure 7.** Schematic nuclear and magnetic structures of $ErFe_2D_5$, showing the $D_1$ and $D_2$ atoms and the orientation of the Er moments at 1.4 K.

**Table 3.** Isomer shift versus Fe(Rh) and quadrupole splitting obtained for $ErFe_2D_5$.

| $T$ (K) $\pm 0.1$ | $\delta$ (mm s$^{-1}$) $\pm 0.01$ | $\Delta$ (mm s$^{-1}$) $\pm 0.01$ |
|---|---|---|
| 295 | 0.35 | 0.37 |
| 4.2 | 0.49 | 0.48 |

we have attempted to fit the 4.2 K data with a narrow sextet corresponding to a moment of about 0.01 $\mu_B$, but not surprisingly the fit is meaningless. This means that down to 4.2 K we observe a zero hyperfine field and that there is no ordered Fe moment at zero field. From figure 8 it is obvious that the linewidth does not change significantly between 295 and 20 K. The hyperfine parameters are given in table 3. The increase in isomer shift upon lowering the temperature (+0.14 mm s$^{-1}$) is predominantly due to the second-order Doppler effect. The increase of the quadrupole splitting (+0.11 mm s$^{-1}$) is indicative of a rise of the electric field gradient at the Fe site when lowering the temperature. This is probably due to the presence of local lattice distortions which are too small to be observed by a powder diffraction experiment. The absence of any magnetic hyperfine splitting indicates the absence of a local field at the Fe site. Thus, the Fe sublattice seems to be in the paramagnetic state down to 4.2 K. Since the Er moments are found to order below 5 K no transferred hyperfine field is observed as well. We have also tried to perform $^{57}$Fe Mössbauer measurements under an applied field to determine if there is an Fe moment but, due to partial deuterium desorption in the mean time, there was

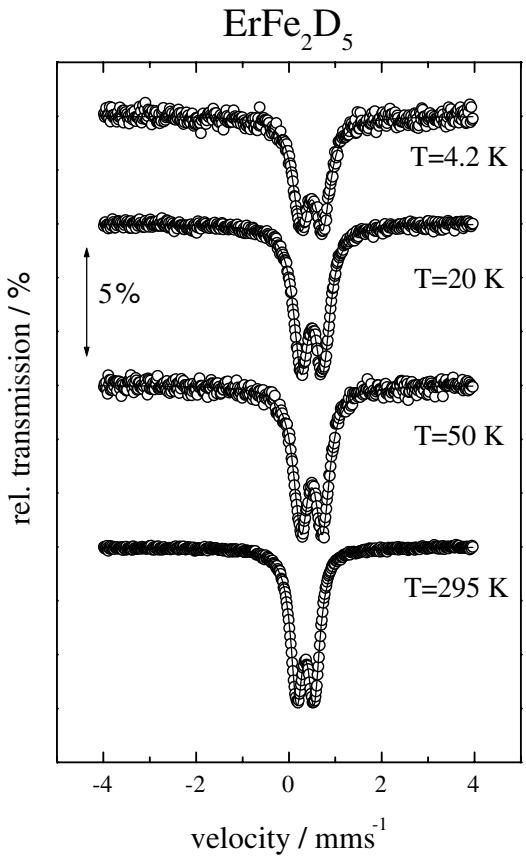


**Figure 8.** $^{57}$Fe Mössbauer spectra of $ErFe_2D_5$ at selected temperatures between 4.2 and 295 K (○) experiment, (—) fit.

a significant mixture of phases and it was not possible to observe the magnetic field effect in the $ErFe_2D_5$ phase.

The temperature variation of the saturation magnetization shows a broad maximum around 150 K and a minimum near 20 K. The large increase of the magnetization (figure 9) at low temperature can be related to the ordering of the Er moments.

Magnetization measurements performed up to 420 K also show a very weak jump at 390 K (figure 9). Since in $YFe_2$ hydrides it was observed that an order–disorder transition from a low symmetry to a cubic C15 type structure occurs above room temperature and is associated with a weak magnetic effect [5, 20], one may assume that this transition is also due to a transition toward a cubic C15 structure.

Upon H absorption in $ErFe_2D_x$ the magnetic behaviour of the Fe sublattice changes from a ferromagnetic state for $x = 0$–3.6 with 1.8 $\mu_B$/Fe to a paramagnetic state for $x = 5$. Such an evolution was already noticed by Dunlap *et al* [21] who have found that the Mössbauer spectra for $^{57}$Fe in $ErFe_2H_{4.1}$ consists also of a doublet down to 4.2 K and that its magnetic ordering temperature should be between 1.5 and 4.2 K with an Fe moment estimated to be about 0.2 $\mu_B$. This strong decrease of the Fe magnetization for large H or D contents could originate either from geometric or electronic factors. In the first assumption this means the existence of a critical Fe–Fe distance above which the Fe moments may be delocalized, like the

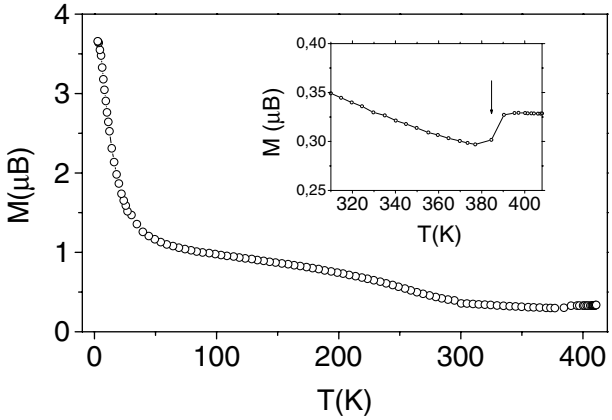


**Figure 9.** Evolution of the magnetization with an applied field of 1.4 T versus temperature. In the inset a zoom of the high temperature magnetization is presented, showing the transition at 390 K.

Mn moments in $RMn_2$ Laves phase compounds [22]. Due to the large volume increase (30%) the calculated Fe–Fe distances increase from 2.574 Å for $x = 0$ to 2.68–2.80 Å for $x = 5$. However, in the $YFe_2D_x$ compounds ($x \leqslant 3.6$), where a wide distribution of Fe–Fe distances exists with Fe–Fe distances even larger than 2.80 Å, the deuterides are still ferromagnetic with an average Fe moment of 1.8 $\mu_B$ [23]. Therefore a strong decrease of the Fe moment in $ErFe_2D_5$ and $YFe_2H_5$ cannot be simply explained by a critical Fe–Fe distance.

The Stoner criterion for the onset of ferromagnetism postulates that the product $I^*n(E_F)$, where $I$ is the exchange integral and $n(E_F)$ is the density of state at the Fermi level, should be larger than one. Therefore a significant decrease of $I$ or $n(E_F)$ can explain the loss of ferromagnetism. Due to the large amount of D atoms one could expect that the additional D electrons would fill the conduction band and consequently reduce $n(E_F)$. On the other hand, each Fe atom is surrounded by about 5 D atoms at distances between 1.6 and 1.8 Å, an influence which can also reduce the exchange integral between the Fe atoms. Band structure calculations are in progress in order to understand the origin of the modification of the Fe–Fe interactions for large hydrogen or deuterium content.

The Er moment in $ErFe_2D_5$ at 1.4 K is 6.6 $\mu_B$ and thus smaller than the value of 8.5 $\mu_B$ found at 4.2 K in $ErFe_2$ which is close to the free ion value of 9 $\mu_B$ [24]. Rhyne *et al* [25] have extrapolated a value of 5 $\mu_B$/Er at 0 K in $ErFe_2H_{3.5}$, whereas Shashikala *et al* [11] reported a value of 6.7 $\mu_B$ for $x = 2$ and 1.13 $\mu_B$ for $x = 4$ at 10 K. This large decrease of the Er moment was attributed to a non-collinearity of the magnetic ordering. However, the authors did not fully refine the NPD patterns but only some magnetic lines, which is not sufficient to check this assumption. In orthorhombic $ErFe_2D_5$, the analysis of the NPD pattern at 1.4 K clearly shows the non-collinearity of the Er moment but this does not explain the reduction of 30% compared to the free ion value. The large variation of the cell parameters below 10 K, near the magnetic ordering temperature of the Er moment at 5 K, could also be an indication that crystal field effects are responsible for the lowering of the Er moments. The weakening of the Er–Er interactions is also observed through the systematic decrease of the magnetic ordering temperature as the D content increases: from 600 K for $x = 0$, 380 K for $x = 2$, 300 K for $x = 3.6$ [26] to 5 K for $x = 5$. This weakening can be attributed to the increase of the Er–Er interatomic distances but also to the influence of interstitial hydrogen (deuterium) atoms.

## 4. Conclusions

The nuclear and magnetic structures of $ErFe_2D_5$ have been investigated versus temperature by neutron diffraction, magnetic and Mössbauer experiments. The orthorhombic structure, which is observed from 1.4 to 300 K, can be attributed to deuterium ordering in 6 $A_2B_2$ and 3 $AB_3$ interstitial sites. The occupancy factors are related to the minimum distance of 2.1 Å due to repulsive interaction between D atoms. The Fe moments are not ordered down to 4.2 K, whereas the Er moments order in a canted magnetic structure below 5 K with 6.6 $\mu_B$ at 1.4 K. The evolution of the magnetic properties of $ErFe_2$ upon H or D absorption shows a decrease of the magnetic ordering temperature, indicating a weakening of all the magnetic interactions.

## Acknowledgments

The authors are very grateful to L Guénée, V Favre-Nicolin and R Cerny (Laboratory of Crystallography in Geneva, Switzerland) for their help in solving the nuclear structure of $ErFe_2D_5$ using the Fox code they have developed.

## References

[1] Kierstead H A 1980 *J. Less-Common Met.* **70** 199
[2] Flanagan T B, Clewley J D, Mason N B and Chung H S 1987 *J. Less-Common Met.* **130** 309
[3] Fruchart D, Berthier Y, de Saxce T and Vulliet P 1987 *J. Less-Common Met.* **130** 89
[4] Fruchart D, Berthier Y, de Saxce T and Vulliet P 1987 *J. Solid State Chem.* **67** 197
[5] Paul-Boncour V, Guénée L, Latroche M, Percheron-Guégan A, Ouladdiaf B and Bourée-Vigneron F 1999 *J. Solid State Chem.* **142** 120
[6] Buschow K H J 1977 *Physica* B+C **86–88** 79
[7] Fish G E, Rhyne J J, Sankar S G and Wallace W E 1979 *J. Appl. Phys.* **50** 2003
[8] de Saxce T, Berthier Y and Fruchart D 1985 *J. Less-Common Met.* **107** 35
[9] Shashikala K, Raj P and Sathyamoorthy A 1996 *Mater. Res. Bull.* **31** 957
[10] Paul-Boncour V, Filipek S M, Percheron-Guégan A, Marchuk I and Pielaszek J 2001 *J. Alloys Compounds* **317/318** 83
[11] Shashikala K, Raj P, Sathyamoorthy A, Chandrasekhar Rao T V, Siruguri V and Paranjpe S K 1999 *Phil. Mag.* B **79** 1195
[12] Paul-Boncour V and Percheron-Guegan A 1999 *J. Alloys Compounds* **293–295** 237
[13] Deryagin A V, Kudrevatykh N V, Moskalev V N and Mushinkov V N 1984 *Phys. Met. Metall.* **58** 96
[14] Viccaro P J, Shenoy G K, Dunlap B D, Westlake D G and Miller J F 1979 *J. Physique* C **2** 198
[15] Paul-Boncour V, Latroche M, Percheron-Guégan A and Isnard O 2000 *Physica* B **276–278** 278
[16] Rodríguez-Carvajal J 1990 *Proc. Congr. Int. Union of Crystallography* p 127
[17] Favre-Nicolin V and Cerny R 2002 *J. Appl. Crystallogr.* **35** 734
[18] Switendick A E 1979 *Z. Phys. Chem.* **117** 89
[19] Westlake D G 1984 *J. Mater. Sci.* **19** 316
[20] Latroche M, Paul-Boncour V, Percheron-Guégan A and Bourée-Vigneron F 1997 *J. Solid State Chem.* **133** 568
[21] Dunlap B D, Shenoy G K, Friedt J M, Viccario P J, Niarchos D, Kierstead H A, Aldred A T and Westlake D G 1979 *J. Appl. Phys.* **50** 7682
[22] Yoshimura K, Shiga M and Nakamura Y 1986 *J. Phys. Soc. Japan* **55** 3585
[23] Paul-Boncour V, Wiesinger G, Reichl C, Latroche M, Percheron-Guègan A and Cortes R 2001 *Physica* B **307** 277
[24] Bargouth M O and Will G 1971 *J. Physique* C **1** 675
[25] Rhyne J J, Fish G E, Sankar S G and Wallace W E 1979 *J. Physique* C **5** 209
[26] Fish G E, Rhyne J J, Sankar S G and Wallace W E 1979 *J. Appl. Phys.* **50** 2003